Electronic Supplementary Material (ESI) for Journal of Materials Chemistry B.

An organic molecular compound for in-situ identification of mitochondrial G-quadruplexes in live cells

Xiaomeng Guo[a,c], Hongbo Chen[a,b], Yan Liu[a], Dawei Yang[a,b], Qian Li[a], Hongyan Du[d], Meirong Liu[a], Yalin Tang*[a,b] and Hongxia Sun *[a]

[a]Beijing National Laboratory for Molecular Sciences, State Key Laboratory for Structural Chemistry of Unstable and Stable Species, CAS Research/Education Center for Excellence in Molecular Sciences, Institute of Chemistry Chinese Academy of Sciences, Beijing, 100190, P. R. China.

[b]University of Chinese Academy of Sciences, Beijing, 100049, P. R. China.

[c]Basic Medical Science, Shenyang Medical college, Shenyang 110034, P. R. China.

[d]Institute of Forensic Science, Ministry of Public Security, Beijing, 100038, P. R. China.

*Email: tangyl@iccas.ac.cn (Y.T.); hongxsun@iccas.ac.cn (H.S.)

Tables of Contents:

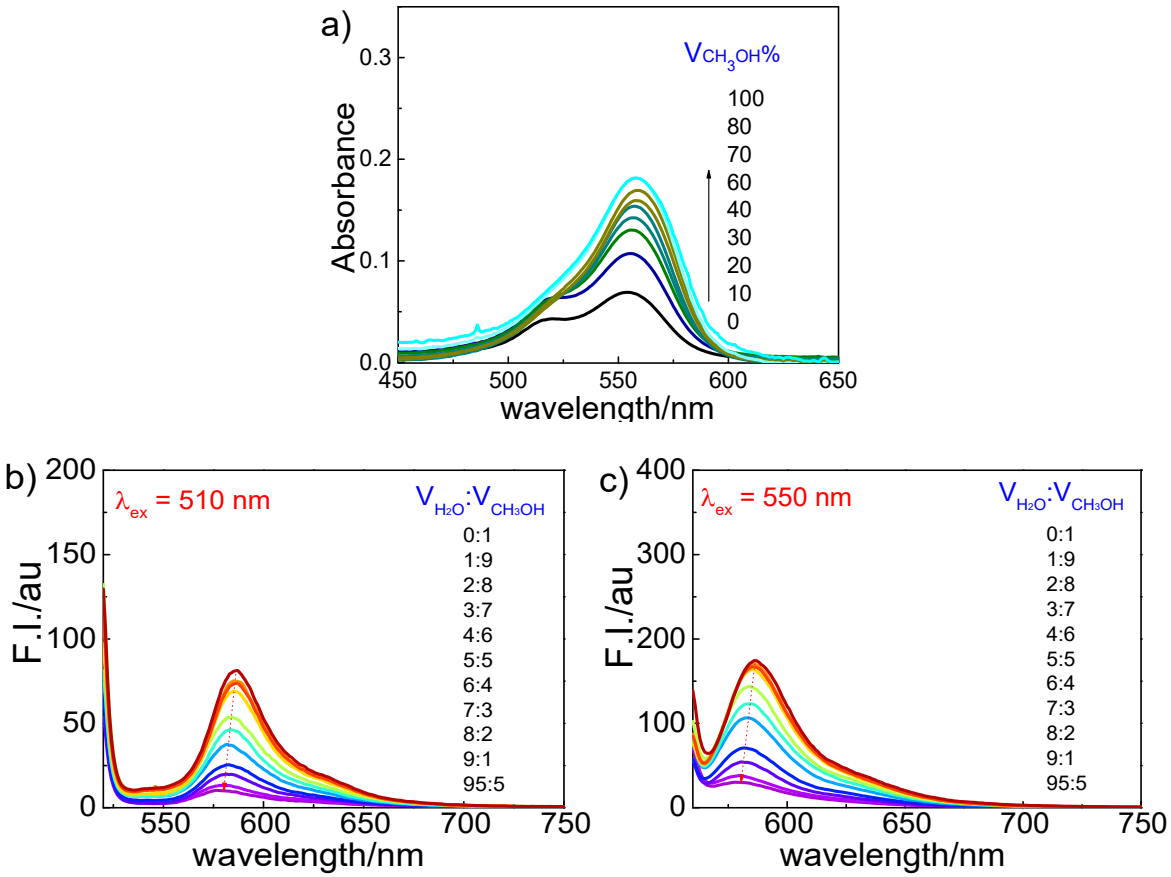

Figure S1. (a) UV-Vis absorption spectra of AMTC (4μM) in aqueous solutions with different methanol content. (b) and (c) Fluorescence spectra of AMTC (4 μM) in aqueous solutions with different methanol content. Both the entrance slit and the exit slit are 5 nm.

It is known that cyanine dyes tend to exist as monomers in the low-polarity solvent methanol. Figure S1 shows that with the increase of methanol content, the monomer absorbance of AMTC increased significantly. Regardless of whether AMTC is excited near the monomer or the dimer, only the fluorescence of the monomer can be detected, and as the content of the dimer increases, the AMTC fluorescence continues to decrease. All these indicate that the dimer does not emit fluorescence.

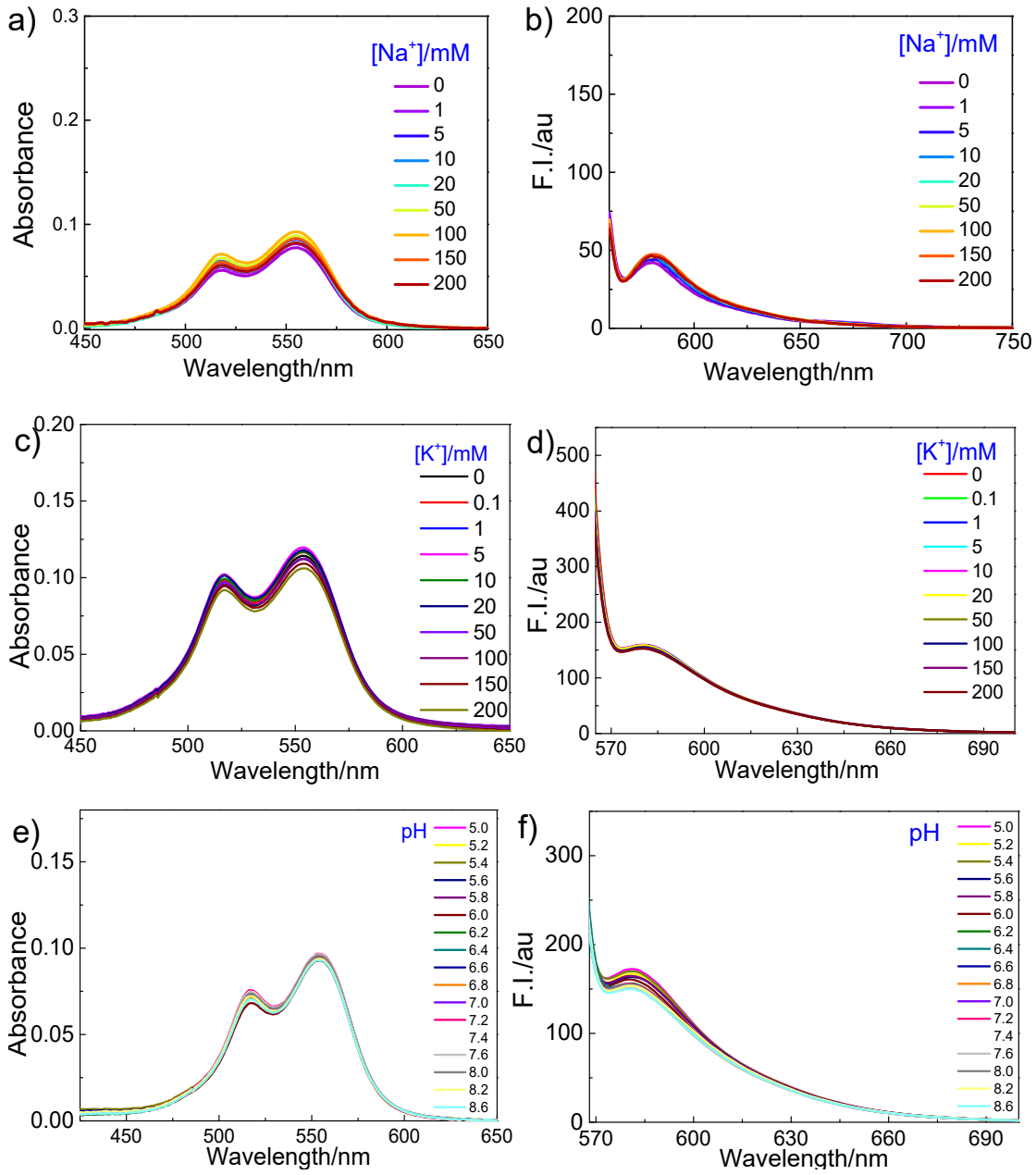

Figure S2. (a) UV-vis absorption and (b) fluorescence spectra of AMTC (4 μM) with Na^+ ranging from 0 to 200 mM in Tris-HCl buffer solution (pH 7.4). Both the entrance slit and the exit slit are 5 nm. (c) UV-vis absorption and (d) fluorescence spectra of AMTC (4 μM) with K^+ ranging from 0 to 200 mM in Tris-HCl buffer solution (pH 7.4). (e) UV-vis absorption and (f) fluorescence spectra of AMTC (4 μM) with pH ranging from 5 to 8.6. λ_{ex}= 550 nm

Table S1. Sequences of the oligonucleotides used in this study and their structures in the buffer solution with 150 mM K^+ and 12 mM Na^+.

Name	Sequence (from5' to 3')	Structure
DNA-Quadruplex		
mt377	GGGGGGGGGGGGTTTGATGTGGGTTGGG	Mito Hybrid G4
mt1015	GGGCTTGATGTGGGGAGGGGTGTTTAAGGG	Mito Hybrid G4
mt10252	GGGTGGGAGTAGTTCCCTGCTAAGGGAGGG	Mito Parallel G4
mt16250	GAAGCGGGGGAGGGGGGGTTTGGTGGAAAT	Mito Hybrid G4
c-myc	AGGGTGGGGAGGGTGGGG	Parallel G4
c-kit	AGGGAGGGCGCTGGGAGGAGGG	Parallel G4
VEGF	GGGCGGGCCGGGGGCGGG	Parallel G4
Bcl-2	GGGCGCGGGAGGAATTGGGCGGG	Hybird G4
Tel22	AGGGTTAGGGTTAGGGTTAGGG	Mixed G4s
TBA	GGTTGGTGTGGTTGG	Antiparallel G4
RNA-Quadruplex		
NRAS	GGGAGGGGCGGGUCUGGG	Parallel RNA G4
Tel22	AGGGUUAGGGUUAGGGUUAGGG	Parallel RNA G4
TRF	CGGGAGGGCGGGGAGGGC	Parallel RNA G4
VEGF	GGAGGAGGGGGAGGAGGA	Parallel RNA G4
Intermolecular G-quadruplex		
TG4T	TGGGGT	Intermolecular G4
T4G4	TTTTGGGG	Intermolecular G4
H12	TTAGGGTTAGGG	Intermolecular G4
G4T2G4	GGGGTTGGGG	Intermolecular G4
i-motif DNA		
c-kit-c	CCCTCCTCCCAGCGCCCTCCCT	i-motif
VEGF-c	CCCGCCCCCGGCCCGCCC	i-motif
Bcl-2-c	CCCGCCCAATTCCTCCCGCGCCC	i-motif
ss-DNA		
S22	TCCCCCCATCCTTACCACCCTC	Single strand
S17	CCCCCCTCCCCATACCC	Single strand
S27	TTTACTTCCTCTCTTTCTTCTTCCCAC	Single strand
ds-DNA		
ds20	CGAATTCGTCTCCGAATTCG	Duplex
ds22	TTCGCGCGCGTTTTCGCGCGCG	Duplex
ds26	CAATCGGATCGAATTCGATCCGATTG	Duplex

mtDNA G-quadruplex

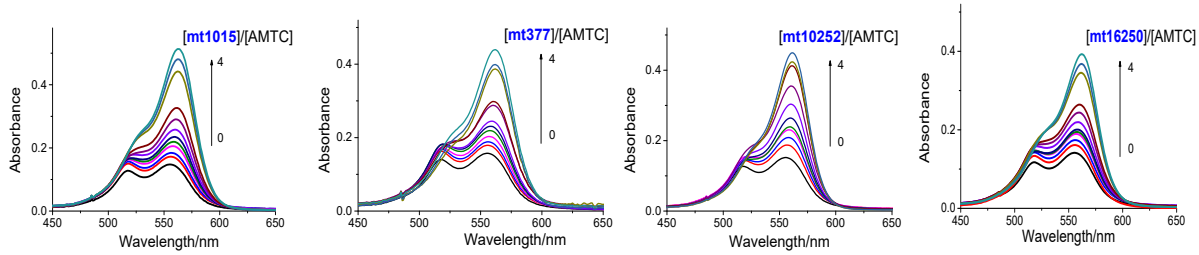

Genomic DNA G-quadruplex

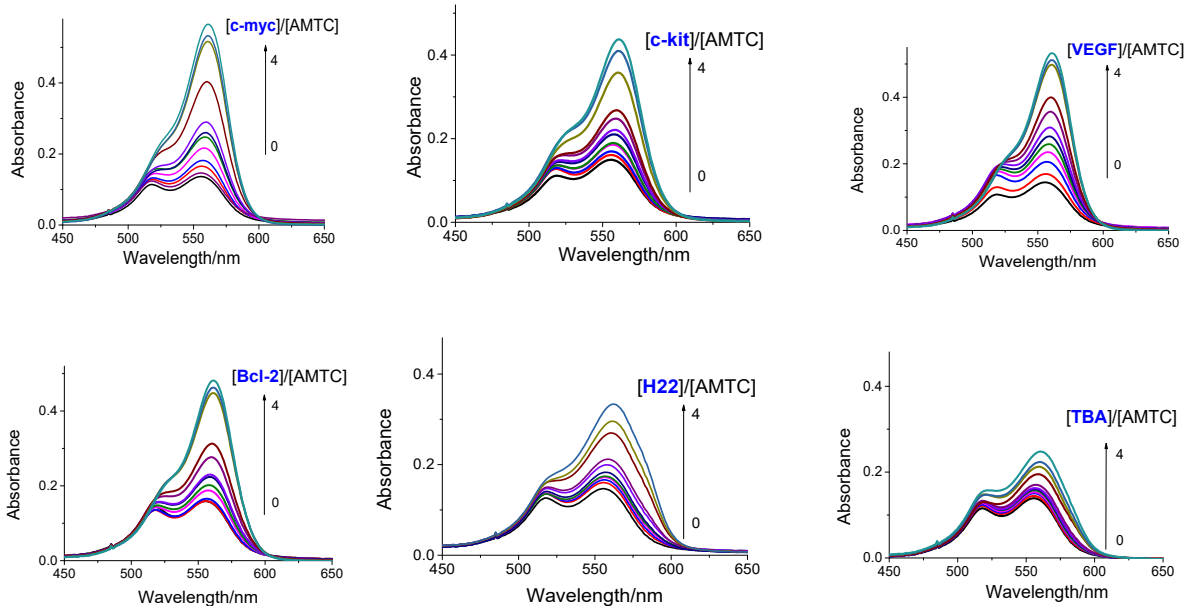

RNA G-quadruplex

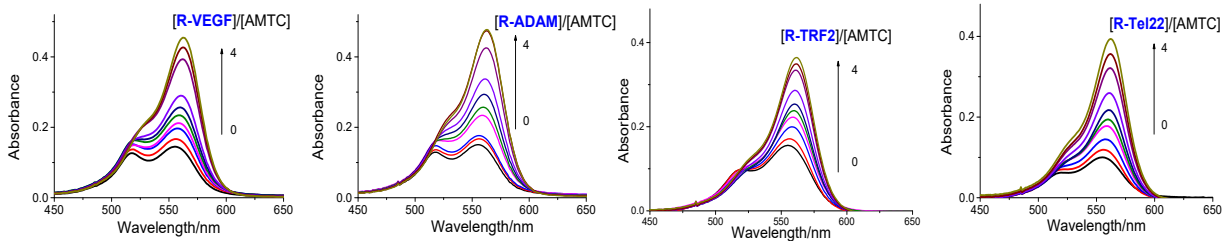

Intermolecular G-quadruplex

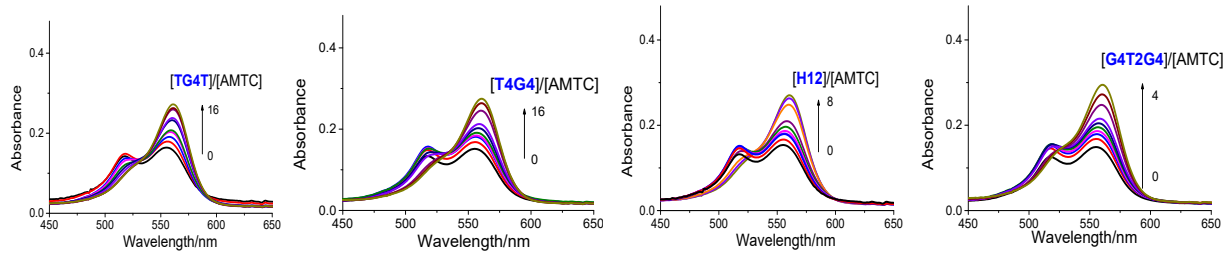

i-Motif DNA

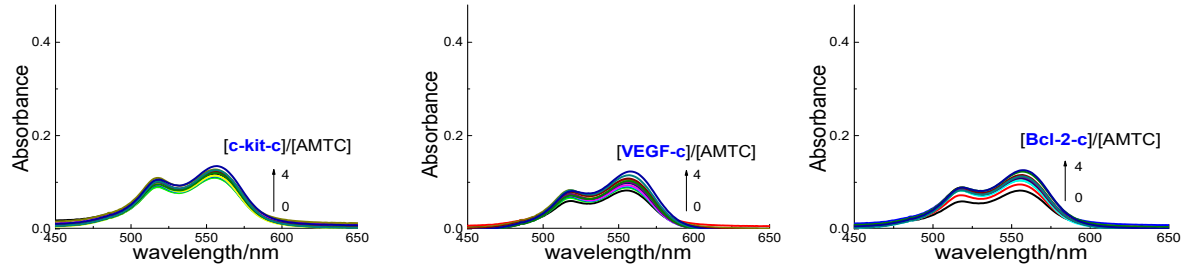

Double-stranded DNA

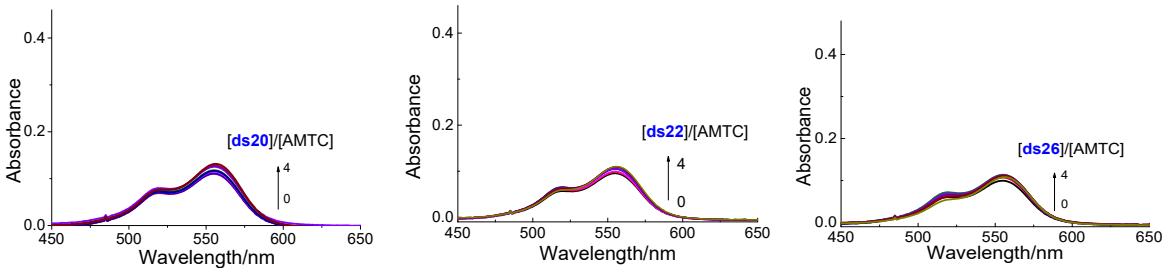

Single-stranded DNA

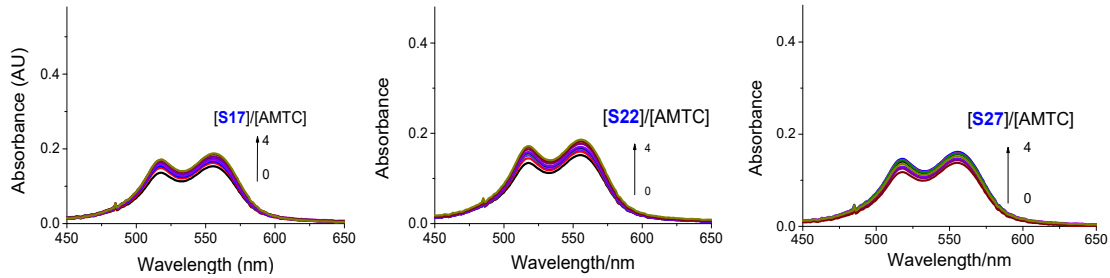

Figure S3. UV-vis absorption spectra of AMTC (4 μM) with increasing concentrations of different DNAs and RNAs in Tris-HCl buffer solution (pH 7.4) containing 150 mM K^+ and 12 mM Na^+. UV-vis absorption spectra of AMTC (4 μM) with i-motif DNAs were measured in Tris-HCl buffer solution (pH 5.2) containing 150 mM K^+ and 12 mM Na^+.

mtDNA G-quadruplex

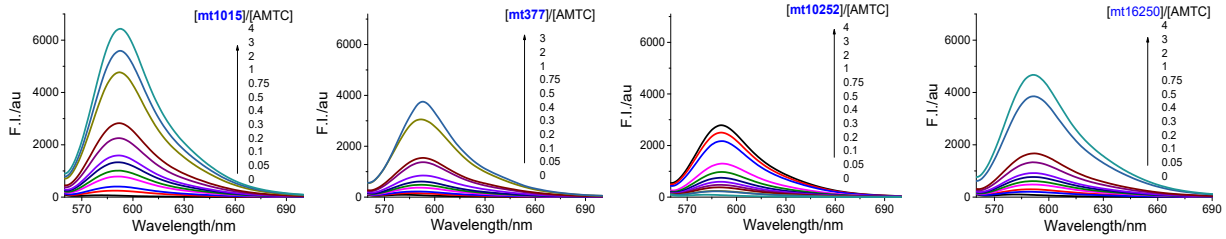

Genomic DNA G-quadruplex

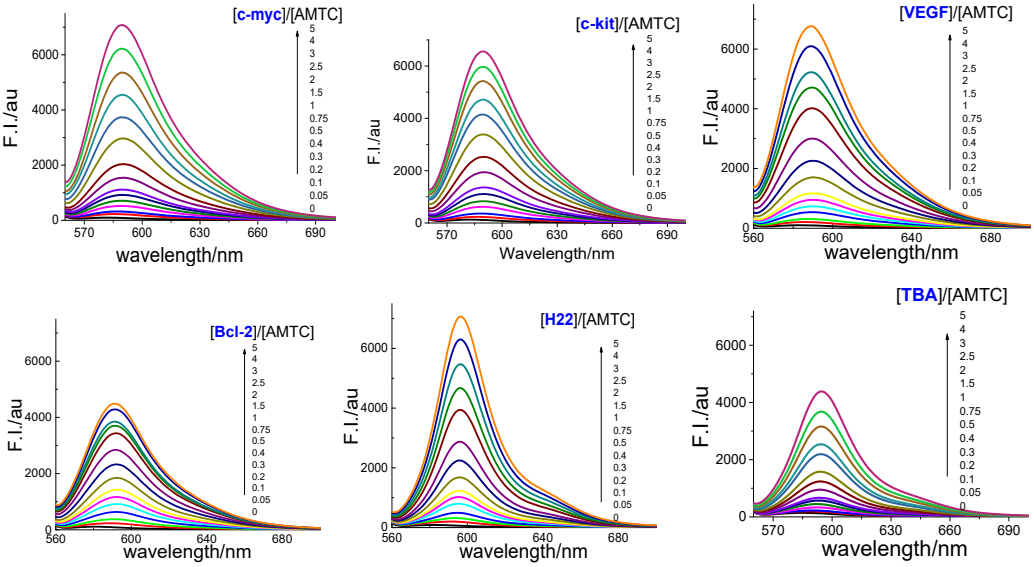

RNA G-quadruplex

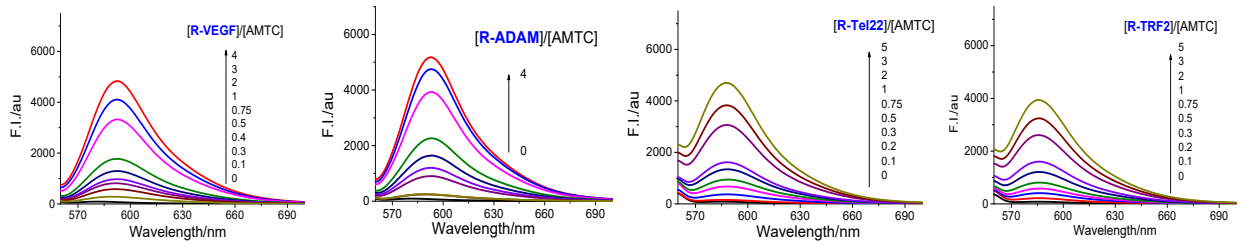

Intermolecular G-quadruplex

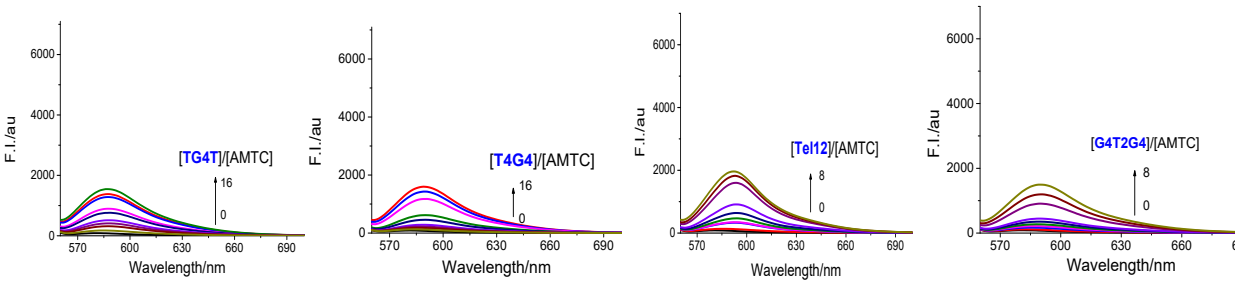

i-Motif DNA

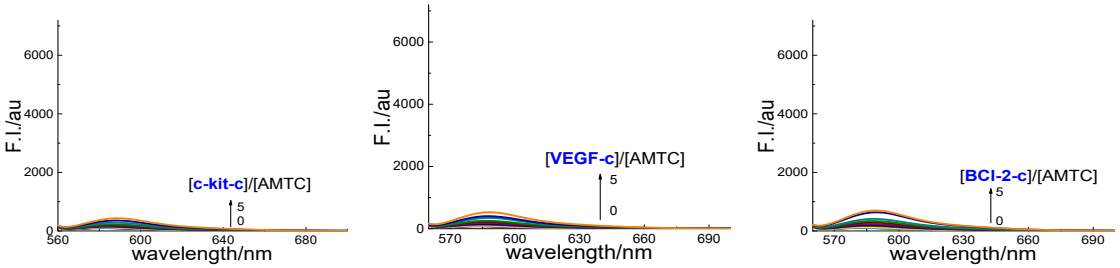

Double-stranded DNA

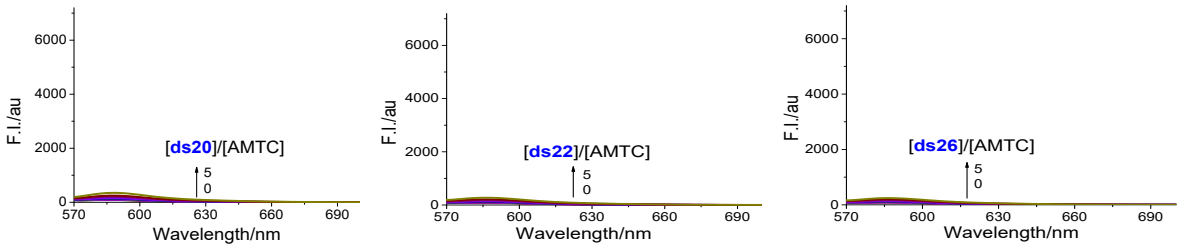

Single-stranded DNA

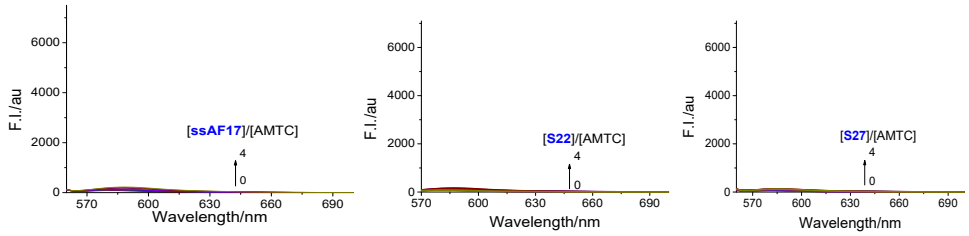

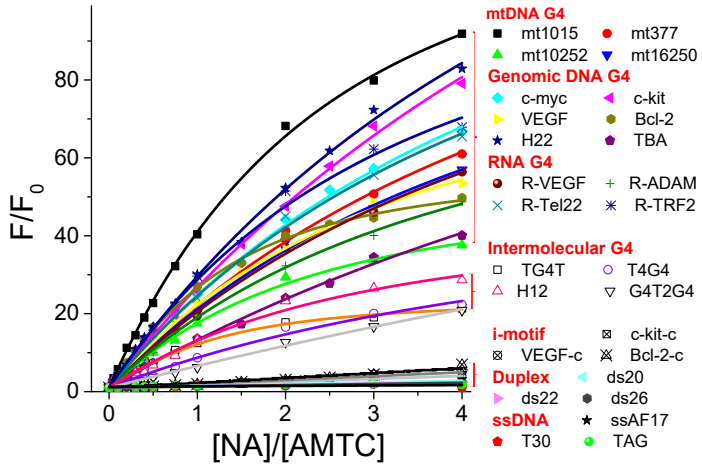

Figure S4. Fluorescence spectra of AMTC (4 μM) with increasing concentrations of different DNAs in Tris-HCl buffer solution (pH 7.4) containing 150 mM K^+ and 12 mM Na^+. Fluorescence spectra of AMTC (4 μM) with i-motif DNAs were measured in Tris-HCl buffer solution (pH 5.2) containing 150 mM K^+ and 12 mM Na^+. λ_{ex}= 550 nm. The plots show the fluorescence emission change of AMTC at 592 nm against the ratio of [NA]/[AMTC]. NA stands for nucleic acid.

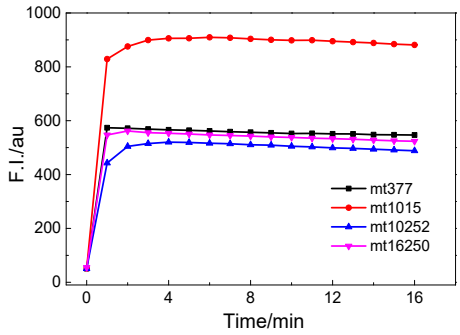

Figure S5. Plots of fluorescence intensity at 590 nm versus time for AMTC interacting with G-quadruplexes. The fluorescence of AMTC (4 μM) with G-quadruplex DNA (4 μM) was measured immediately after adding the G-quadruplex DNA in Tris-HCl buffer solution (10 mM, pH 7.2) with 150 mM K^+ and 12 mM Na^+. λ_{ex}= 550 nm, Voltage = 400V.

The results show that within 1 minute after the addition of G-quadruplexes, the AMTC fluorescence increased sharply and reached a maximum value, supporting the immediate response of AMTC.

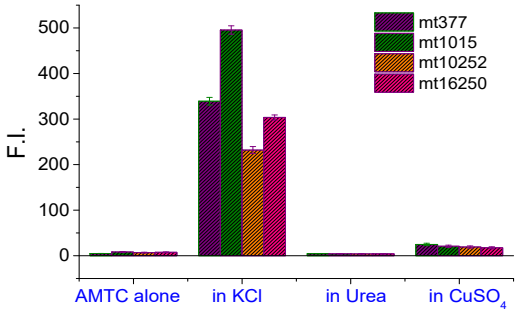

Figure S6. The fluorescence intensity at 590 nm of 4 μM AMTC with 8 μM different G-quadruplexes under KCl or quadruplex-unfolding conditions (2 M Urea or 1 mM $CuSO_4$). λ_{ex} = 550 nm, voltage = 400V.

Once the G-quadruplex structure was decomposed by urea and $CuSO_4$ (1,2), AMTC fluorescence was remarkably quenched, demonstrating that the enhanced fluorescence can only be maintained by G-quadruplexes.

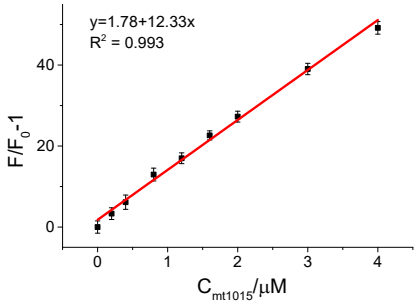

Figure S7. Fluorescence change of AMTC (4 μM) at 592 nm with increasing concentrations of mt1015 G-quadruplexes in Tris-HCl buffer solution (10 mM, pH 7.2) with 150 mM K^+.

The linearity plot showed that the enhanced emission intensity was linear in the range of 0-4 μM with a correlation coefficient of R^2 = 0.993. The detection limit was evaluated to be 3.4 nM according to the conventional IUPAC rule CDL= 3σ /S, where σ = 0.014 is the standard deviation of blank measurement and S=12.33 is the slope between fluorescence intensity ratio (F/F_0-1) and concentration of mt1015.

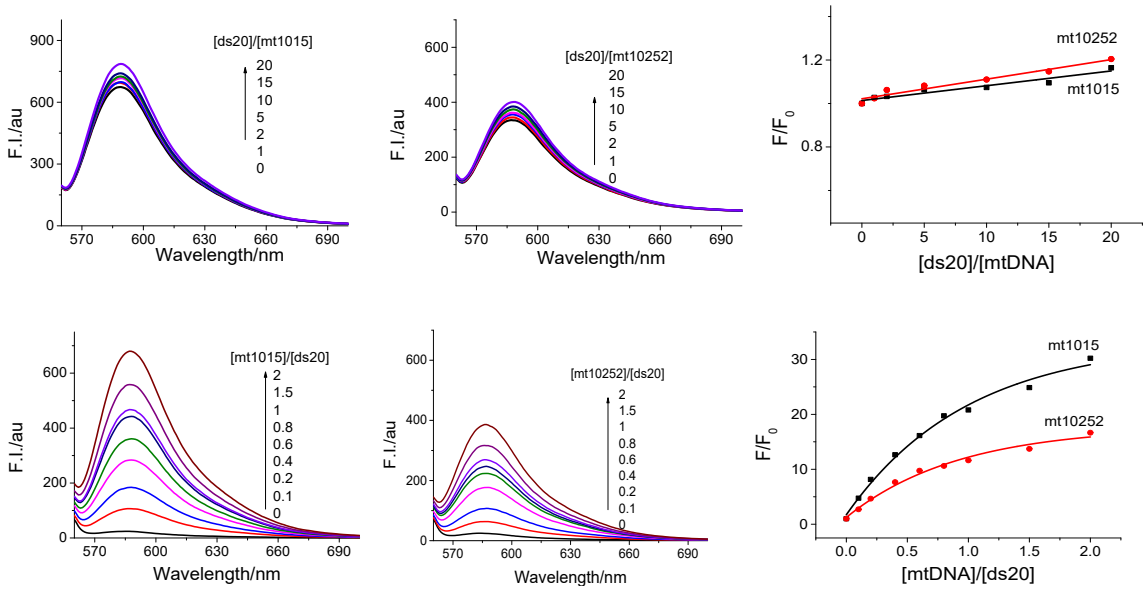

Figure S8. (Up) Competitive fluorescence titration of AMTC (2 μM) and mtDNA G-quadruplex (2 μM) complexes with increasing amounts of duplex DNAs (ds20). (Down) Competitive fluorescence titration of AMTC (2 μM) and ds20 (2 μM) complexes with increasing amounts of mtDNA G-quadruplexes. All samples were measured in Tris-HCl buffer solution (10 mM, pH 7.2) containing K^+ (150 mM) and Na^+ (12 mM).

With the addition of duplex DNA, the fluorescence of AMTC-quadruplex adducts increased slightly. Even though 20 molar equivalents of duplex DNA were added, the fluorescence enhancement was within 20%. Reverse titration data also showed that AMTC remains sensitive to G-quadruplexes when duplex DNA is present.

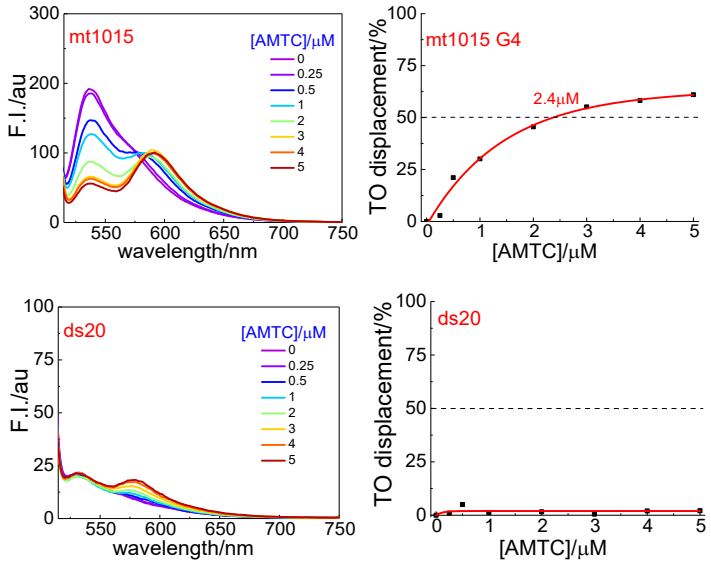

Figure S9. Fluorescent intercalator displacement assay of TO (0.5 μM) by AMTC in the presence of mt1015 G-quadruplex (0.25 μM) and ds20 duplex DNA (0.25 μM) in Tris-HCl buffer solution (10 mM, pH 7.4) with K^+(150 mM) and Na^+(12 mM). λex = 501 nm. Only the TO on the G-quadruplex structure has been competed by AMTC, meaning that AMTC has good selectivity to the G-quadruplex structure.

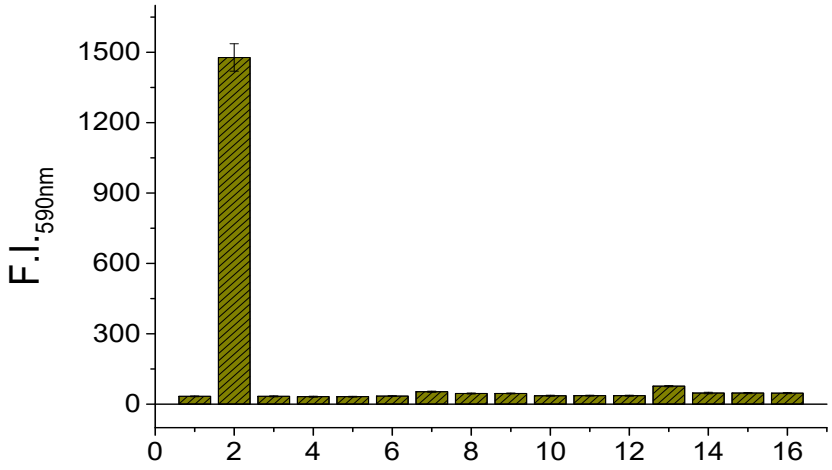

Figure S10. (A) Specificity of AMTC (4 μM) to G-quadruplex structures. (1) Blank, (2) mt377 (10 μM), (3) Glutamate (1 mM), (4) arginine (1 mM), (5) serine (1 mM), (6) alanine (1 mM), (7) aspartate (1 mM), (8) cysteine (1 mM), (9) reduced glutathione (5 mM), (10) glucose (1 mM), (11) Mg^{2+} (2 mM), (12) Ca^{2+} (2 mM), (13) Zn^{2+} (100 μM), (14) Cu^{2+}(100 μM), (15) vitamin C (1 mM), (16) thrombin (20 nM), All the samples were measured in Tris-HCl buffer solution (10 mM, pH 7.2) containing K^+ (150 mM) and Na^+ (12 mM). λ_{ex}= 550 nm.

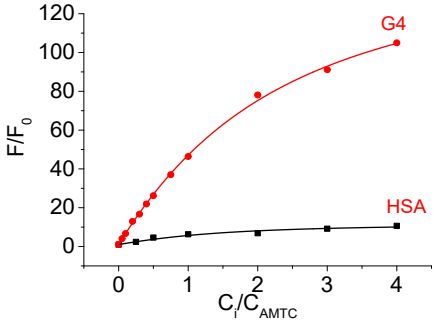

Figure S11. AMTC fluorescence intensity change with the mt1015 G-quadruplex (G4) and HSA titration in Tris-HCl buffer solution (pH 7.4) containing 150 mM K^+ and 12 mM Na^+. λ_{ex}= 550 nm.

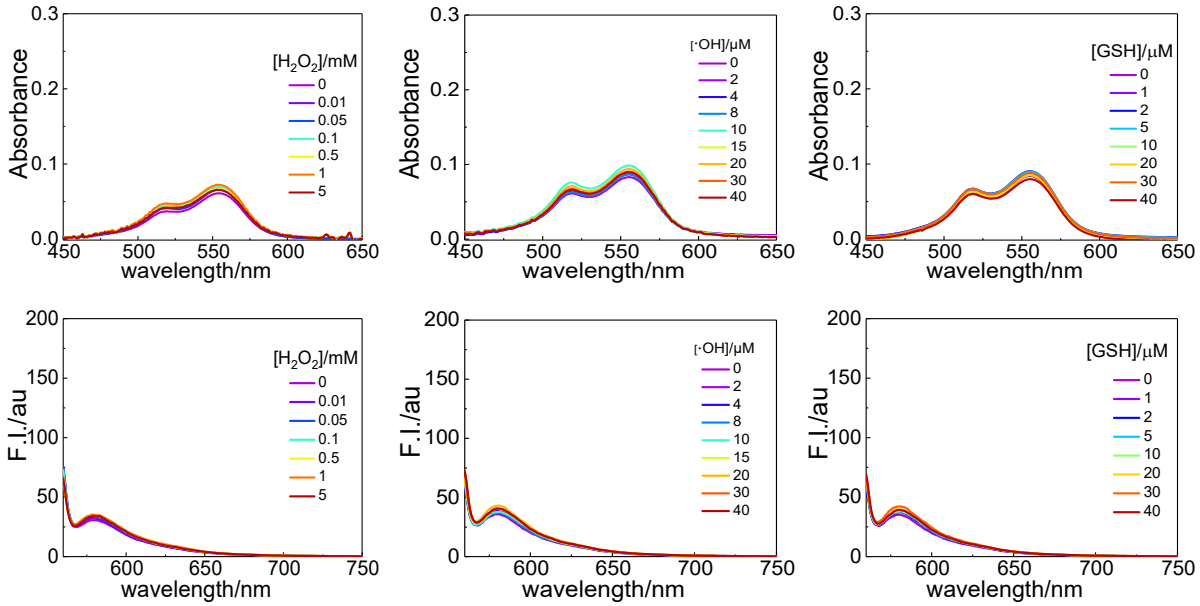

Figure S12. UV-Vis absorption spectra and fluorescence spectra of AMTC (4 μM) with increasing concentrations of H_2O_2, ·OH, and GSH in Tris-HCl buffer solution (pH 7.4) containing 150 mM K^+ and 12 mM Na^+. Hydroxyl radicals were generated by Fenton reaction. The ratio of Fenton's reagent was ($[H_2O_2]/[Fe^{2+}$-EDTA] = 10:1), and the concentration of ferrous ions was approximately that of hydroxyl radicals. Different concentrations of Fenton's reagent were added to the buffer solution containing 4μM AMTC, and the reaction was carried out for 30 min.

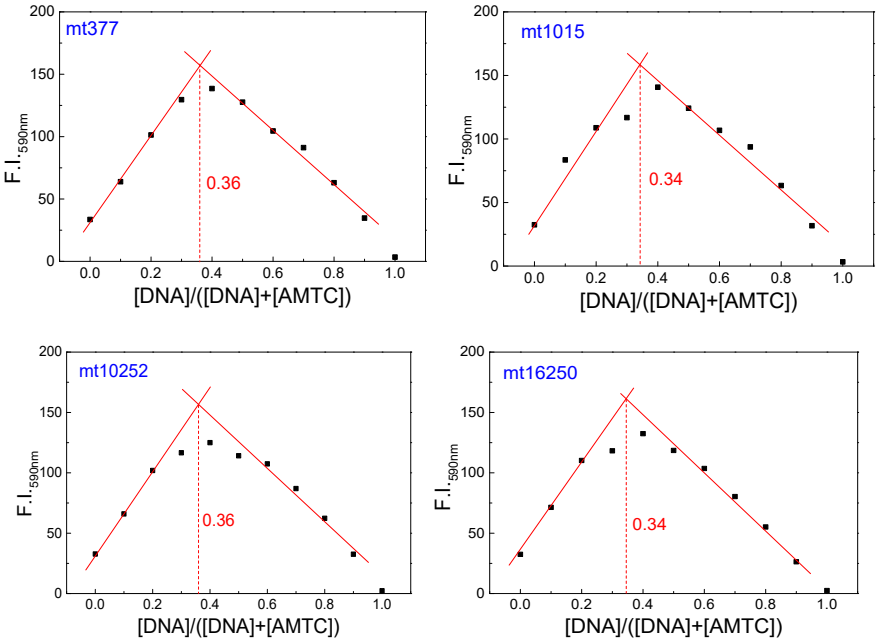

Figure S13. Job plot analysis for the binding stoichiometry of AMTC to the mtDNA G-quadruplex structures in Tris-HCl (10 mM, pH 7.2) with 150 mM K^+ and 12 mM Na^+. The total concentration of DNA and AMTC is 2 μM. All samples were prepared Excitation was set at 550 nm and emission was measured at 590 nm. The point of intersection for the Job plot is near 0.34, showing a 2:1 stoichiometry of AMTC binding to these G-quadruplexes.

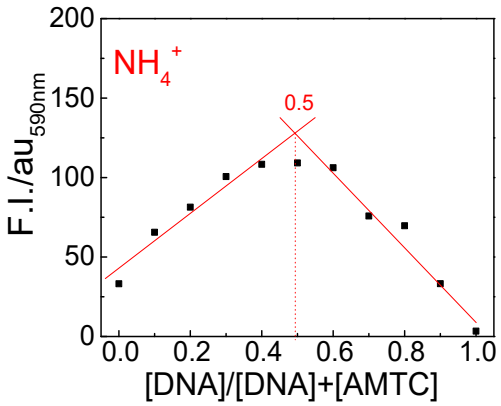

Figure S14. Job plot analysis for the binding stoichiometry of AMTC to the mt1015 G-quadruplex in mixed solutions of methanol and 50 mM ammonium acetate (volume ratio 1:4, pH 6.8). The total concentration of mt1015 DNA and AMTC is 2 μM. All samples were prepared Excitation was set at 550 nm and emission was measured at 590 nm. The point of intersection for the Job plot is near 0.5, showing a 1:1 stoichiometry of AMTC binding to these G-quadruplexes.

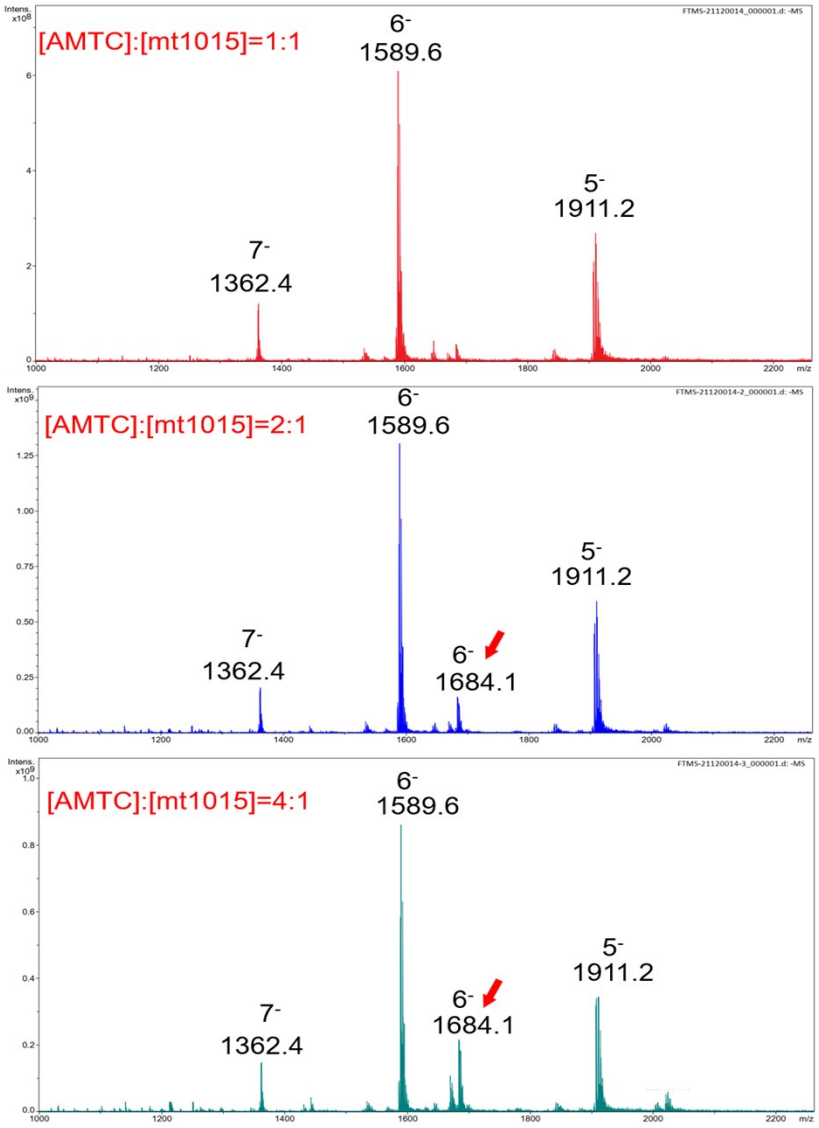

Figure S15. ESI-HRMS of AMTC and mt1015 G-quadruplex (4 μM) and mixed in different molar ratios. Sample preparation: mt1015 was dissolved in 200 mM ammonium acetate solution (pH = 6.8) to prepare a DNA stock solution with a concentration of 100 μM. Heated at 90 ℃ for 5 min, then slowly cooled to room temperature, and left it stand overnight. The mt1015 DNA (Mw=9510) and AMTC (Mw=565) were mixed in molar ratios of 1:1, 1:2 and 1:4, respectively, and diluted with methanol: 50 mM ammonium acetate (volume ratio 20:80) solution to a final DNA concentration of 4 μM.

m/z 1362.4 corresponds to the seven-charge mass spectrum peak, that is $[mt1015+2NH_4^+-9H^+]^{7-}$, m/z1589.6 corresponds to the six-charge mass spectrum peak of $[mt1015+2NH_4^+-8H^+]^{6-}$, m/z1911.2 corresponds the five-charge mass peak of $[mt1015+2NH_4^+-7H^+]^{5-}$. With the increase in AMTC concentration, a new six-charged mass spectrum peak with m/z of 1684.1 appeared, which was estimated to be $[mt1015+2NH_4^+-8H^++AMTC]^{6-}$, corresponding to the 1:1 binding ratio of mt1015 and AMTC.

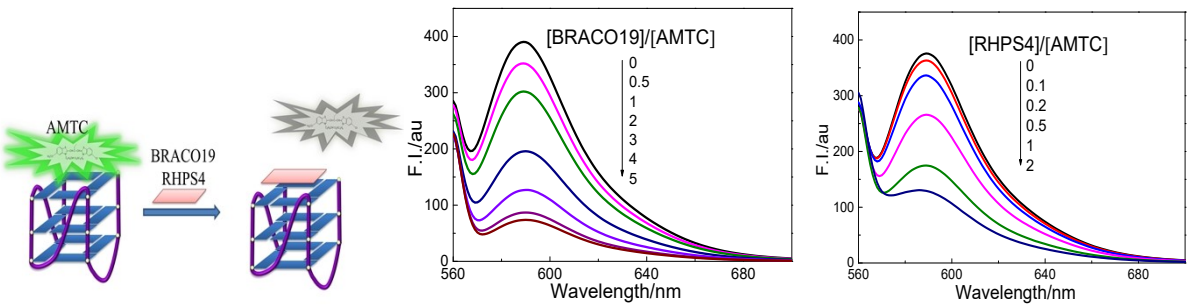

Figure S16. Fluorescence spectra of AMTC (2 μM)-mt1015 G-quadruplexes (2 μM) with increased concentration of BRACO19 and RHPS4 in Tris-HCl (10 mM, pH 7.2) buffer solution with 150 mM K^+ and 12 mM Na^+. λex= 550 nm.

Both BRACO19 and RHPS4 are classical G-quadruplex ligands, and they are reported to be stacked on the end planes of G-quadruplex structures (3,4). After treatment with BRACO19 and RHPS4, a sharp decrease in the original fluorescence of the AMTC/G-quadruplex adducts was observed, indicating that AMTC may have the same G-quadruplex binding sites as BRACO19 and RHPS4.

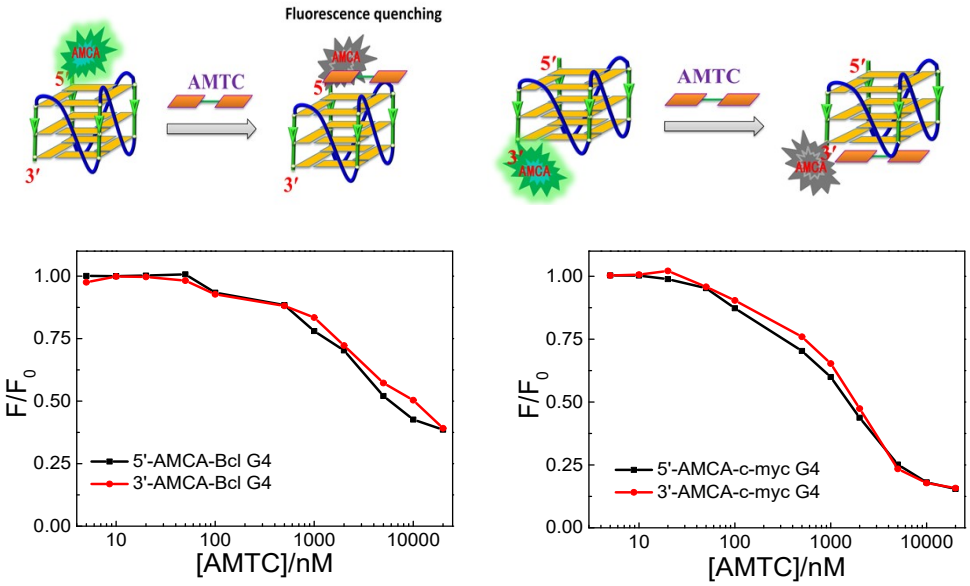

Figure S17. Schematic representation of ligands towards G-quartet selectivity analysis. The ratio (F/F_0) of fluorescence intensity of AMCA-labelled Bcl-2 and c-myc G-quadruplexes (0.2 μM) as a function of AMTC concentration in 20 mM Tris-HCl (pH 7.2) with 150 mM K^+ and 12 mM Na^+. F_0 and F represent the fluorescence intensity of AMCA -quadruplex at 450 nm before and after interacting with AMTC, respectively. λex= 353 nm. Bcl-2 and c-myc represent hybrid-type and parallel G-quadruplex, respectively. The AMCA fluorescence at both the 5 'and 3' ends was quenched, indicating that AMTC may simultaneously bind to the two terminal planes of G-quadruplexes (5).

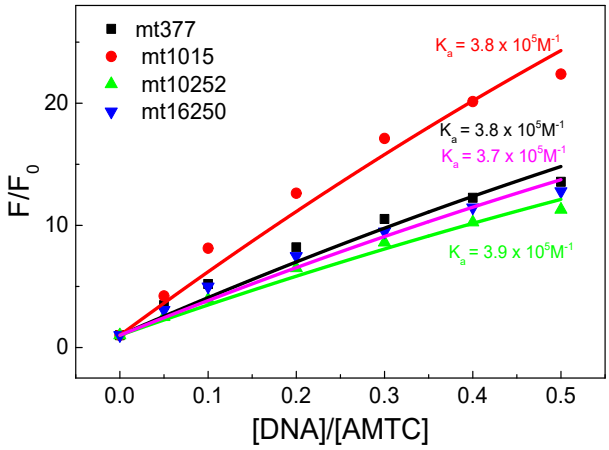

Figure S18. Binding curves at 500 nm for AMTC (4 μM) with different DNA G4s in 20 mM Tris-HCl buffer (pH 7.4) containing 150 mM K^+ and 12 mM Na^+. The data from the fluorimetric titrations were analyzed by nonlinear fitting to eq (6) $y = 1 + \frac{Q-1}{2}\left[A + 1 + x - \sqrt[2]{(A+1+x)^2 - 4x}\right]$ according to the independent-site model (7), in which $y=F/F_0$ (F is the fluorescence intensity upon addition of indicated DNA concentration and F_0 is the integral fluorescence intensity of AMTC in the absence of G-quadruplexes), $Q=F_{max}/F_0$ (F_{max} is the fluorescence intensity upon saturation), $A = (K_a C_{AMTC})^{-1}$, $x = nC_{G4s}(C_{AMTC})^{-1}$ and n is the putative number of binding sites on a given G-quadruplex substrate. The parameters, Q and A, were found by Levenberg−Marquardt fitting routine in the Origin 9.0 software.

mtDNA is in a single-stranded state

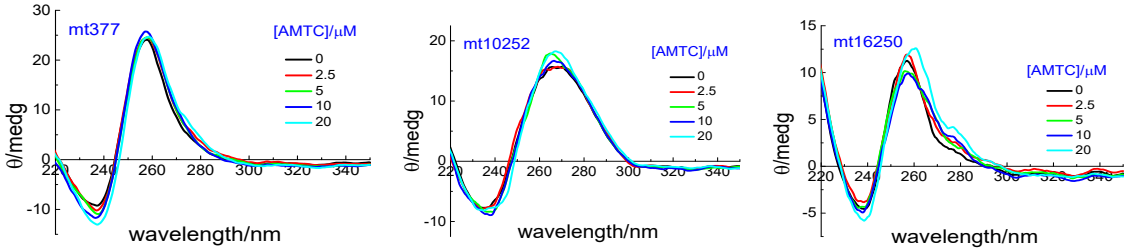

mtDNA exists as a G-quadruplex

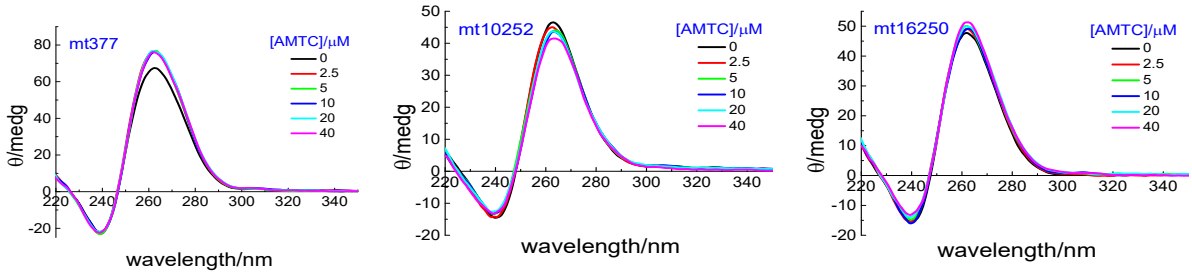

Figure S19. CD spectra recorded for various mtDNA (5 μM) with increasing concentrations of AMTC. mtDNA exists in a single-stranded state in Tris-HCl buffer solution (20 mM, pH 7.4) without K^+, and exists in G-quadruplex in Tris-HCl buffer solution (20 mM, pH 7.4) with 150 mM K^+.

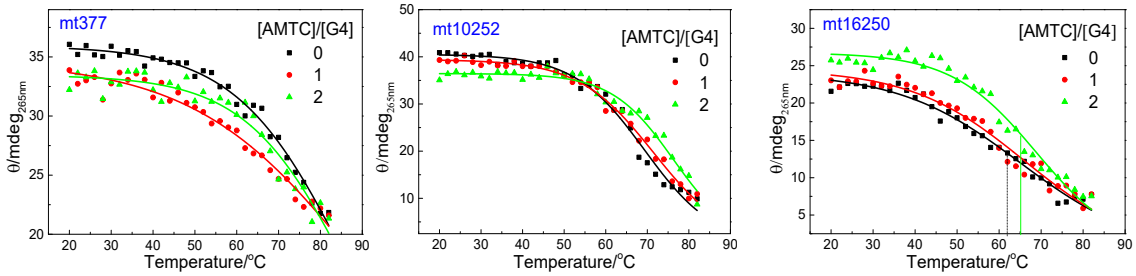

Figure S20. Molar ellipticity at 265 nm as a function of temperature for DNA G-quadruplexes (4 μM) without and with AMTC (4 and 8 μM) in 10 mM Tris-HCl (pH 7.4) with 150 mM K^+ and 12 mM Na^+.

Cytotoxicity assay. Cytotoxicity assays were carried out using HeLa and MCF-7 cells. Cell viability was determined using MTT assay. 5000−6000 cells per well were seeded in a 96-well plate and incubated for 16 h in a cell incubator for adherence. AMTC dissolved in methanol was added to cells at the final concentration of 0.5, 1, 5, 10, and 20 μM and incubated for 96 h. MTT diluted by DMEM medium (10%) was added to each well after the removal of culture media and incubated for 4 h. Following that, the absorbance was measured at 492 nm on a plate reader after the removal of culture media and adding DMSO. Cell viability was determined as VR = $(A-A_0)/(As-A_0) \times 100\%$, where A is the absorbance of the experimental group, As is the absorbance of the control group, and A_0 is the absorbance of the blank group (no cells).

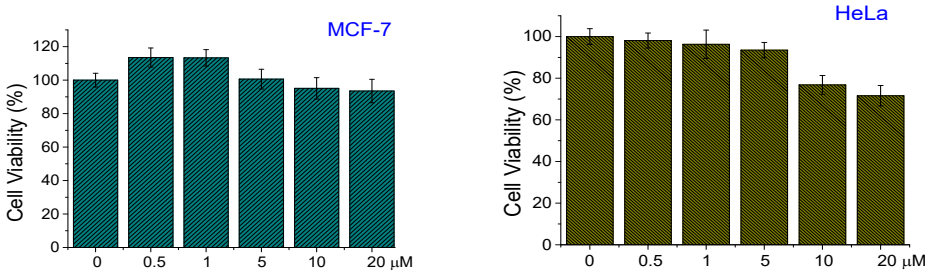

Figure S21. Cell viability of HeLa and MCF-7 cells in the presence of different concentrations of AMTC (0−20 μM) after 96 h incubation. The viability of the cells without AMTC is defined as 100%. The results are expressed as the mean ± standard derivation of three separate measurement.

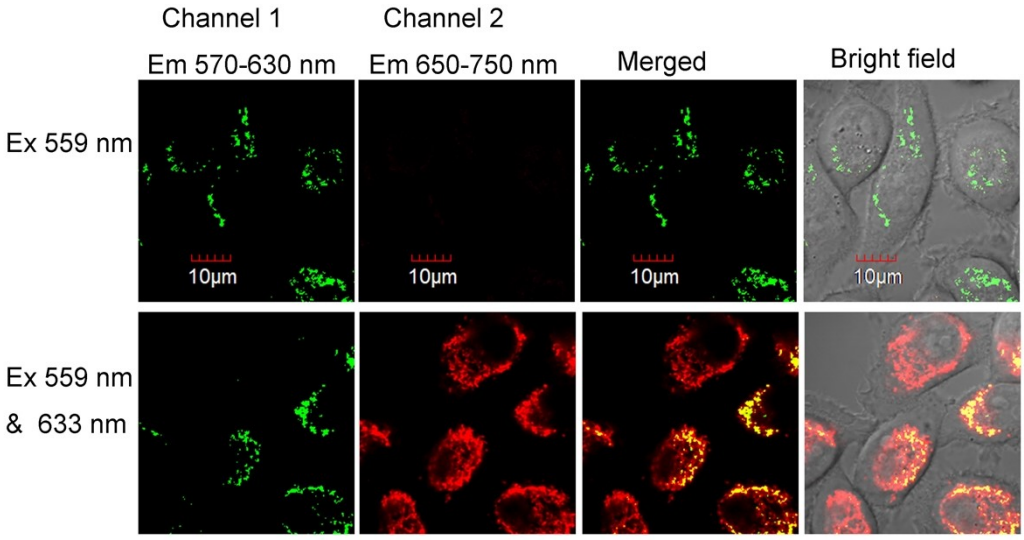

Figure S22. CLSM images of live MCF-7 cells stained with AMTC (2 μM, Ex 559 nm) and MitoTracker Deep Red (50 nM, Ex 633 nm). When excited at 559nm, AMTC did not produce fluorescence interference at 650-750nm.

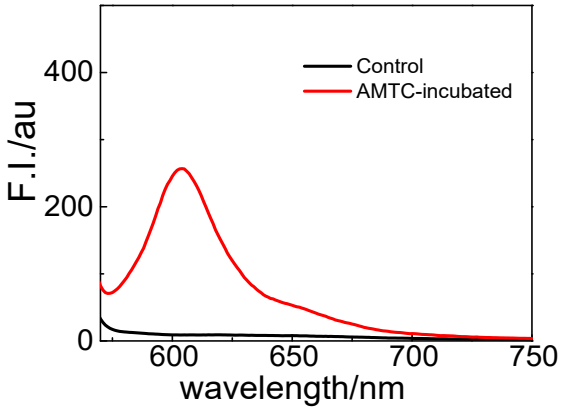

Figure S23. Fluorescence spectra of AMTC in mitochondria extract. The extraction of mitochondria was carried out in accordance with the product instructions by using Cell mitochondria isolation kit (CS0201, Leagene Biotechnology Co., Ltd. Beijing, China). 10^7 HeLa cells were incubated without and with AMTC (20 μM) for 30 min and then washed with pre-cooled PBS, centrifuged at 1000g at 4 °C for 5 min, and the supernatant was discarded. The sediment was resuspended in 1-2ml of pre-chilled Mitochondria Lysis buffer and placed in an ice bath for 10 min. Transferred the cell suspension to a Dounce homogenizer and homogenize 15 times. Took the homogenate, immediately added the same amount of wash buffer, gently inverted and mixed several times. Centrifuged at 1300g for 5 min at 4°C to remove nuclei, unbroken cells and large membrane debris. Transferred the supernatant to a clean centrifuge tube, centrifuged at 1000g at 4°C for 5 min, and repeated twice. Transferred the supernatant to a clean centrifuge tube, centrifuged at 12000～15000g at 4°C for 15 min, repeated once. Discarded the supernatant and suspended the sediment in 1mL PBS with Triton X-100 (0.2%) and NP-40 (0.3%). The fluorescence spectrum is excited at 550nm, and both the entrance slit and the exit slit are set to 5nm.

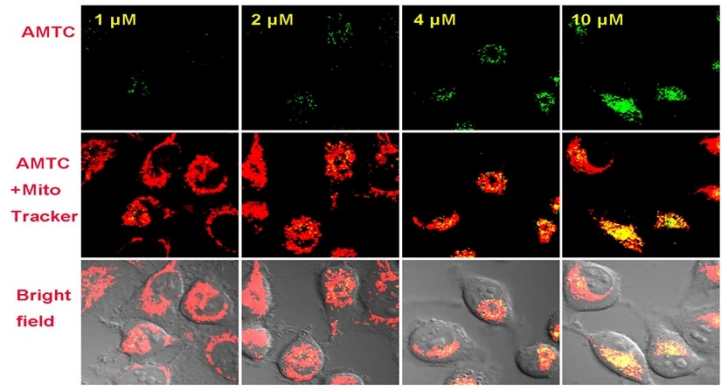

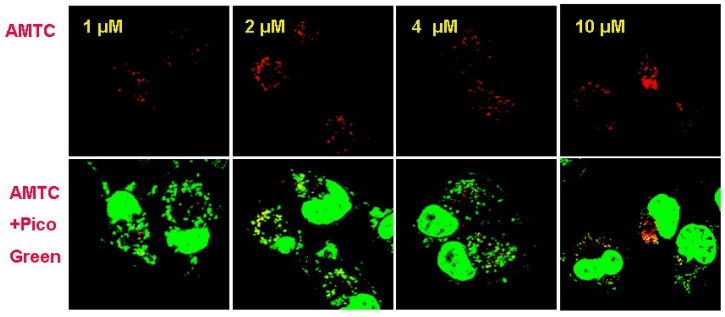

Figure S24. CLSM images of live MCF-7 cells stained with AMTC (1, 2, 4, 10 μM, Ex 559 nm), MitoTracker Deep Red (50 nM, Ex 633 nm) and PicoGreen (2μL, Ex 488 nm). As the AMTC concentration increases, the overlap coefficient of AMTC and MitoTracker Deep Red also increases (from 0.88 to 0.96).

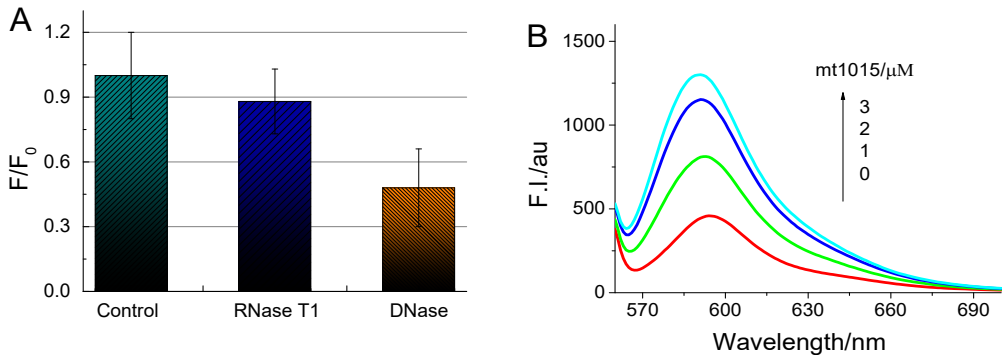

Figure S25. (A) Changes in the fluorescence intensity of AMTC (2 μM) in PBS (pH 7.4) containing mitochondrial lysate after DNase I and RNase T1 treatment. (B) Fluorescence spectra of AMTC (2 μM) with increasing concentrations of mt1015 G-quadruplexes in PBS (pH 7.4) containing mitochondria lysate. λ_{ex}= 550 nm

The extraction of mitochondria was the same as that in Figure 23. For enzyme treatment experiments, the mitochondria lysate in PBS as digested with 0.1 mg/mL DNase I (Thermo Fisher Scientific) or 1 mg/mL RNase T1 (Thermo Fisher Scientific) at 37 °C for 1 h. In the mtDNA G-quadruplex addition experiment, AMTC and different concentrations of mt1015 were sequentially added to the mitochondrial lysate solution for spectral measurement.

References

1. Ueda, Y. M. et al. (2016) Effects of trimethylamine N-oxide and urea on DNA duplex and G-quadruplex. *Sci. Technol. Adv. Mat.*, **17**, 753–759.
2. Ma, L., Han, X., Xia, L., et al. (2020) A label-free G-quadruplex-based fluorescence assay for sensitive detection of alkaline phosphatase with the assistance of Cu^{2+}. *Spectrochim Acta A Mol. Biomol. Spectrosc.*, **227**, 117607.
3. Machireddy, B., Sullivan, H.-J. and Wu, C. (2019) Binding of BRACO19 to a telomeric G-quadruplex DNA probed by all-atom molecular dynamics simulations with explicit solvent. *Molecules,* **24**, 1010.
4. Gavathiotis, E., Heald, R.A., Stevens, M.F.G. and Searle, M.S. (2003) Drug recognition and stabilisation of the parallel-stranded DNA quadruplex d(TTAGGGT)$_4$ containing the human telomeric repeat. *J. Mol. Biol.*, **334**, 25–36.
5. Le, D.D., Antonio, M.D., Chan, L.K.M. and Balasubramanian, S. (2015) G-quadruplex ligands exhibit differential G-tetrad selectivity. *Chem. Commun.*, **51**, 8048–8050.
6. Xie, X., Choi, B., Largy, E., et al. (2013) Asymmetric distyrylpyridinium dyes as red-emitting fluorescent probes for quadruplex DNA. *Chemistry,* **19**, 1214–1226.
7. Stootman, F.H., Fisher, D.M., Rodger, A. and Aldrich-Wright, J.R. (2006) Improved curve fitting procedures to determine equilibrium binding constants. *Analyst,* **131**, 1145–1151.